A Precipitation Model for Multi-Component Multi-Phase Systems in Nickel-Base Superalloys

C. Sommitsch[a], E. Kozeschnik[b], G. Wasle[b], B. Buchmayr[b]

[a]Boehler Edelstahl GmbH & Co KG, Kapfenberg, Austria
[b]Institute for Materials Science, Welding and Forming, Graz University of Technology, Graz, Austria

Abstract

A process model developed by the authors for the calculation of the microstructure evolution of nickel-base alloys during the hot forming process in a rolling mill helps to optimise the rolling process and aids in achieving the desired microstructure. The simulation of the particle development during and after a hot forming process is based on the numerical Kampmann-Wagner model. The chemical driving forces for precipitation are obtained from the thermodynamic equilibrium module of the computer program 'MatCalc'. The multicomponent diffusion coefficients are evaluated from the atomic mobilities that are compiled in the mobility-database of the DICTRA software.

Keywords: Nickel-base-alloys; Superalloys; Precipitation; Simulation; Carbides; Gamma-Prime

1. Introduction

In the last 15 years, several numerical models for the microstructural simulation of industrial processes, such as heat treatment or hot forming processes, have been developed. There are commercial FE-computing programs available that can describe the evolution of the grain structure and the phase fractions based on semi-empirical models (e.g. DEFORM^{TM}-HT). However, such models can not handle complex alloy systems like nickel-base alloys, where simultaneous precipitation of carbides and the γ'-phase can occur within the temperature range for hot deformation. These processes strongly affect the microstructural evolution, i.e. recrystallization and grain growth.

The present model [1] couples an extended Kampmann-Wagner [2] approach for nickel-base alloys with the program MatCalc [3]. The latter is utilized for the evaluation of the driving forces for precipitation, the equilibrium phase compositions and the multicomponent diffusion coefficients.

2. Thermodynamic Model and Multicomponent Diffusion

The equilibrium module of the thermokinetic software package MatCalc is based on the minimum total Gibbs Free Energy principle

$$G_m = \sum_i f^i \cdot G_m^i = Minimum \qquad (1),$$

where G_m is the molar Gibbs free energy of the system, G^i_m is the molar Gibbs free energy of a phase i and f^i is the corresponding phase fraction. The thermodynamic formalism describing G^i_m is based on the sublattice model [4] and the thermodynamic parameters are read from

available commercial databases, i.e. the nickel-base database [5]. The software structure has recently been described in detail in reference [6].

The chemical diffusion coefficients D that are needed to simulate the growth and coarsening kinetics of precipitates are evaluated from the model of Andersson and Ågren [7]. The required mobility data is evaluated from the mobility database of the software package DICTRA [8].

3. Precipitation Model

The precipitation model described here is based on the numerical Kampmann-Wagner model [2], which is derived from classical nucleation and growth theory [9]. Phase separation in solid alloys often occurs as the thermally activated migration of atoms through a phase boundary. Hence, the free energy changes with the free volume energy ΔG_V (chemical formation energy), because of the formation of new phase volume (energy gain), and the free surface energy, because of the formation of new interface area (energy loss). In case of coherent particles, the elastic strain energy ΔG_ε, due to the lattice misfit of the matrix and the particle, must also be considered. The change of the free energy during a nucleation process is therefore [10]

$$\Delta G = -V\left(\Delta G_V - \Delta G_\varepsilon\right) + A\gamma_{\alpha\beta} \tag{2},$$

where V is the volume, A is the surface area of the nucleus and $\gamma_{\alpha\beta}$ is the phase boundary energy (α: matrix, β: precipitated phase). Inserting for the energy contributions in equation (2) and building the extremum for ΔG yields the critical nucleus radius

$$R^* = \frac{2\gamma_{\alpha\beta}}{\Delta G_V - \Delta G_\varepsilon} \tag{3}.$$

For heterogeneous nucleation at dislocations and at interfaces, the phase boundary energy can be set to a smaller value due to the fact that the energy barrier for nucleation at inhomogeneities is lower [11]. With equations (2) and (3), the critical work of formation ΔG^* is

$$\Delta G^* = \frac{16\pi\gamma_{\alpha\beta}^3}{3\left(\Delta G_V - \Delta G_\varepsilon\right)^2} \tag{4}.$$

With these terms, an expression for the nucleation rate J can be derived [12]

$$J(t) = J_s \exp\left(-\frac{\tau}{t}\right) = Z\,\beta^*\,N_0 \exp\left(-\frac{\Delta G^*}{kT}\right)\exp\left(-\frac{\tau}{t}\right) \tag{5},$$

where J_s is the stationary nucleation rate which is reached after the nuclei (clusters) that formed have a stable size with negligible probability of dissolution. τ indicates the incubation time. N_0 designates the number of potential nucleation sites per unit volume and β^* the rate at which solute atoms from the matrix with mean concentration c join the nucleus. In the present model, both N_0 and β^* depend on the nucleation site and are either related to the lattice parameter (homogeneous nucleation), to the grain size (nucleation at grain boundaries) or to the dislocation density (strain induced nucleation) [13]. The growth rate of an over-critical spherical nucleus is given by

$$\frac{dR}{dt} = \frac{c(t) - c_R}{c_p - c_R}\frac{D}{R} \tag{5},$$

where c_p, $c(t)$ and c_R are the concentrations of the solute in the precipitate, in the matrix and at the interface boundary, respectively. The latter is given in terms of the Gibbs-Thompson equation [14]:

$$c_R(R) = c_e \exp\left(\frac{2\gamma_{\alpha\beta}}{R_g T}\frac{V_\beta}{R}\right) \tag{7},$$

where R_g is the universal gas constant, c_e is the equilibrium concentration of the solute in the matrix and V_β is the molar volume of the precipitate phase.

4. Numerical Model

In the present model (fig. 1), thermodynamic equilibrium is calculated with MatCalc for each time step and in a phase loop the precipitation behaviour of all phases is examined.

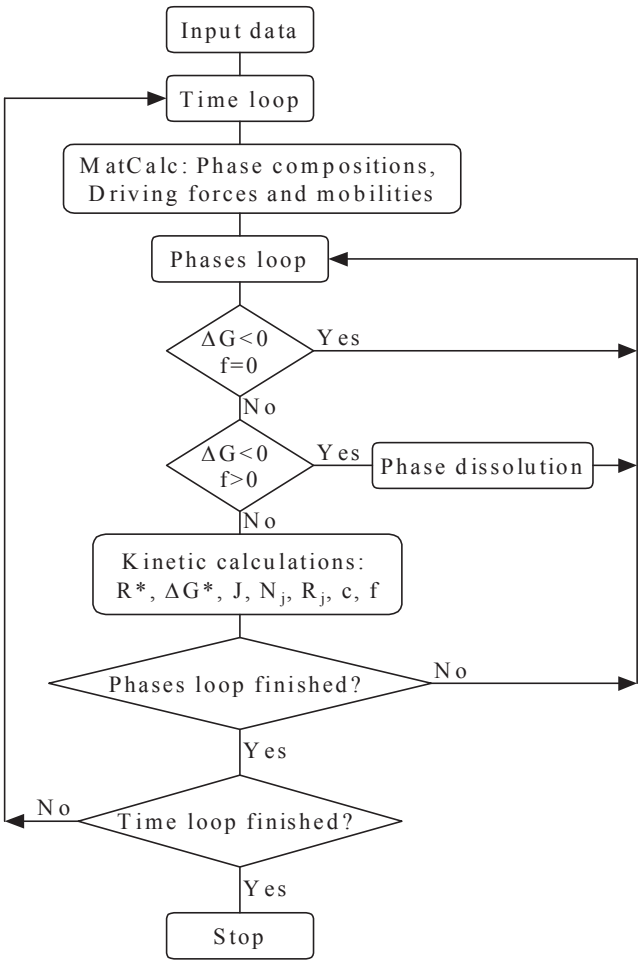

Fig. 1. Flow chart of the numerical model.

The kinetic computation begins after the equilibrium atomic concentrations of the phases, the chemical driving forces and the chemical diffusion coefficients of each diffusing component are read into the kinetics module. If the driving force for the precipitation of a phase is positive, nucleation and particle growth is calculated, otherwise dissolution. At the end of the phase loop, the new phase amounts are passed to the thermodynamics module and the new equilibrium conditions for the next time step are calculated.

In each time step, $N(t)$ particles with mean radius $R(t)=R^*$ nucleate according to equations (2)-(5). The continuous size distribution $f(R,t)$ is separated into small logarithmic intervals $[R_{j+1},R_j]$ with N_j particles. Subsequently, the new radii $R_j(t+\Delta t)$ are evaluated with equation (6). Numerical models such as the Kampmann-Wagner model treat nucleation, growth and coarsening as concomitant processes. Coarsening reactions start to occur as soon as the supersaturation of the matrix decreases so far that the critical radius R^* becomes greater than the radius of the smallest particles. In this case, the smallest particles become thermodynamically unstable and begin to dissolve. Each time step Δt is completed with the calculation of the mean concentration of the solute atoms in the matrix $c(t)$

$$c(t) = c_0 - \left(c_p - c_e\right)\sum_{j=1}^{N} \frac{4\pi}{3} \overline{R}_j^3 N_j \qquad (8),$$

where c_0 is the concentration at $t=0$ and $\overline{R}_j$ and N_j are the mean radius and the particle density of the j^{th} size interval, respectively.

The following simplifications are made in the model: The calculated phases normally consist of several elements with variable equilibrium concentrations dependent on temperature. It seems to be useful for the simulation to consider only the major constituents. For each phase, the supersaturated elements, which are mainly responsible for the particle growth, have to be defined (Cr and C for the carbides, Al and Ti for γ'). Also, for the diffusivity computations, the atom type which governs the bulk or grain boundary diffusion has to be determined (Cr for the carbides, Al for γ'). The model does not consider the varying coherency and, thus, the changing phase boundary energy during the early stages of precipitation. If there are stable particles (e.g. coarse primary carbides) that do not dissolve, they are treated as phases with constant phase fraction. An automatic time step procedure was developed to adapt to the different time-scales of nucleation, growth and coarsening, where appropriate time step widths are estimated from both the nucleation rate and the precipitated phase amount per time step.

The evaluated phase fractions and the chemical composition of each phase also affect the evolution of the grain structure (and vice versa), which is calculated in a separate module [1]. The interaction of the grain structure and the precipitation model mainly concerns the following processes: Nucleation of particles at grain boundaries and strain induced nucleation at dislocations; dragging forces on moving high angle grain boundaries (Zener drag, solute drag) and interaction of moving dislocations with particles and solute atoms. Corresponding information is given in detail in reference [1].

5. Experimental

Experiments were performed to confirm the simulation results of the carbide precipitation model on measured phase fraction data. Samples of Böhler L306 VMR (Alloy 80A) were cut from hot rolled pieces, thus ensuring a completely recrystallized, fine-grained and homogenous

microstructure. Solution heat treatment was carried out at 1220°C for 210 seconds, followed by water quenching in order to retain a supersaturated solid solution. The short annealing time was chosen to avoid grain growth. Ageing was done at 800°C for 3, 10, 25 and 50 hours, again followed by water quenching. The grain boundary precipitates $M_{23}C_6$ were studied by optical and scanning electron microscopy (SEM) techniques. The specimens were electrolytically polished in distilled water (60%) and caustic soda (40%) at room temperature for 30 seconds at 250mV prior to examination. Other etching methods were tested for comparison.

The quantitative investigation of $M_{23}C_6$ was carried out with a specialized image analysing software. M(C,N) carbides were investigated in the same way to check this method as the MC-fraction should stay almost stable at 800°C over ageing time.

6. Results

The model predictions were verified on the alloy system Ni-12at%Al [15] and Ni-14at%Al [16,17] by comparing with literature data. Fig. 2 shows the particle density N and the nucleation rate J for T=550°C. The measured data were obtained by atom probing field ion microscopy (FIM, [17]) and high resolution transmission electron microscopy (HREM, [16]). When coarsening starts, the particle density begins to decrease due to the dissolution of unstable particles with a radius smaller than the current critical radius. In the simulations, the nucleation process was assumed to be homogeneous.

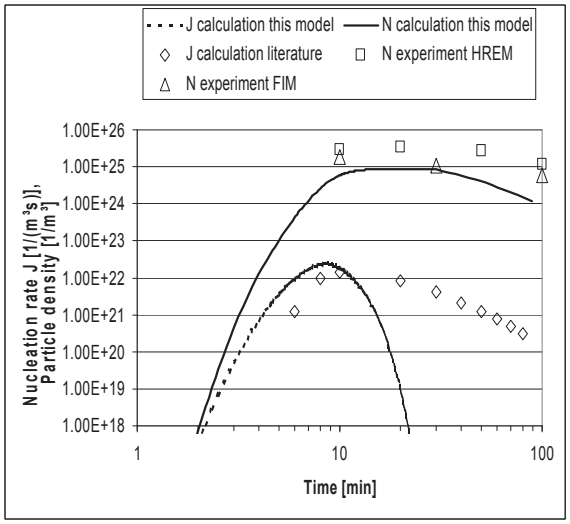

Fig. 2. Particle density N and nucleation rate of γ'-particles during an isothermal heat treatment at 550°C in the alloy system Ni-14at% Al. Experimental data for N [16,17] and calculated values for J [17] compared with calculated data for N and J (this model).

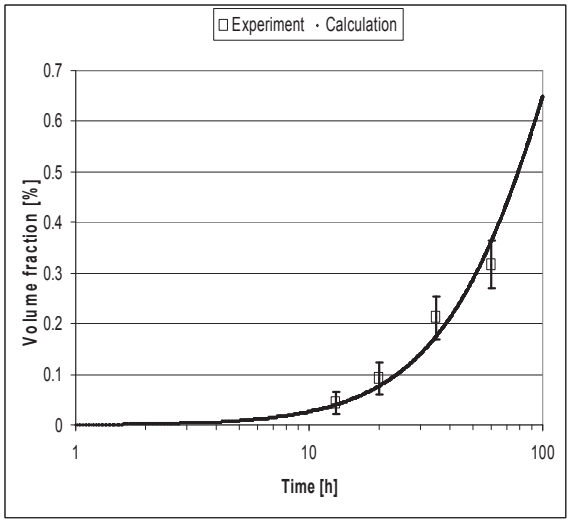

Fig. 3. Volume fractions of chromium carbides $M_{23}C_6$ in Alloy 80A at 800°C after various annealing times (Solid line: Calculated. Boxes: Experimental).

Fig. 3 shows the comparison of calculated and measured phase amounts of the carbide $M_{23}C_6$ in the Alloy 80A. The equilibrium volume fraction of $M_{23}C_6$ was calculated to be approximately 1%. If nucleation occurs preferentially at grain boundaries, the number of potential nucleation sites per unit volume depends on the grain size. This fact is taken into account in equation (5) by setting appropriate values for N_0 [13]

$$N_0 = \frac{1}{a^2 L} \tag{9},$$

where L denotes the average grain size (120μm in this case).

7. Conclusions

The described numerical procedure represents a general model for the simulation of the time-dependent size distribution of precipitate phases in nickel-base superalloys. The nucleation, growth and coarsening processes occurring in these alloys are modelled in an iterative manner. Currently, the model is embedded in a general microstructure model that is coupled to a commercial FE-computer program for the simulation of hot forming processes.

8. References

[1] C. Sommitsch, Ph.D. Thesis, Institute for Materials Science, Welding and Forming, Graz University of Technology, Graz, 1999.
[2] R. Kampmann, R. Wagner, in: Decomposition of Alloys: The Early Stages, P. Haasen (Ed.), Pergamon, Oxford, United Kingdom, 1984, p. 91.
[3] E. Kozeschnik, Ph.D. Thesis, Institute for Materials Science, Welding and Forming, Graz University of Technology, Graz, 1997.
[4] M. Hillert, L.-I. Staffansson, Acta Chem. Scand. 24 (1970) 3618.
[5] N. Saunders, Phil. Trans. 351A, 1995, 543.
[6] E. Kozeschnik, B. Buchmayr, in: Mathematical Modelling of Weld Phenomena 6, H. Cerjak, H.K.D.H. Bhadeshia (Eds.), Institute of Materials, London, 2000, in print.
[7] J.-O. Andersson, J. Ågren, J. Appl. Phys. 72, 1992, 1350-1355.
[8] J.O. Andersson, L. Hoeglund, B. Joensson, J. Agren, in: Fundamentals and Applications of Ternary Diffusion, G.R. Purdy (Ed.), Pergamon Press, NY, 1990, pp. 153-163.
[9] R.D. Doherty, in: Physical Metallurgy, R.W. Cahn, P. Haasen (Eds.), Elsevier, Amsterdam, 1983, p. 942.
[10] A.K. Sinha, in: Ferrous Physical Metallurgy, Butterworth, Stoneham, 1989, p. 121.
[11] S. Park, J. Jonas, Met. Trans. 23A, 1992, 1641.
[12] A.H. Cottrell, in: Report on Strength of Solids, The Physical Society, London, 1948.
[13] M. Militzer, W. Sun, J. Jonas, in: Microstructure and Properties of Microalloyed and other Modern High Strength Low Alloy Steels, M. DeArdo (Ed.), Pittsburgh, 1991.
[14] R. Wagner, R. Kampmann, in: Mater. Sci. Technol., vol. 5, P. Haasen (Ed.), VCH, Weinheim, 1990, p. 213.
[15] S. Xiao, P. Haasen, Acta Met. Mater. 39, 1991, 651.
[16] H. Wendt, P. Haasen, Acta Met. 31, 1983, 1649-1659.
[17] P. Haasen, R. Wagner, Met. Trans. 23A, 1992, 1901-1914.